Supporting Information

Balana et al. 10.1073/pnas.1018645108

SI Materials and Methods

Preparation of Rabbit Polyclonal Anti-SNX27 Antibody. A polyclonal SNX27 antibody was generated in rabbits immunized against peptide containing the first 18 residues of the N terminus of SNX27 followed by tyrosine (sequence MADEDGEGIHPSTPHRNGY) following a standard protocol. The obtained rabbit antibody is a pan-SNX27 antibody, because it recognizes the N terminus in both SNX27a and SNX27b. Antiserum was collected at multiple time points to sample across the immune response and assessed using Western blot analysis.

Fluorescent Immunohistochemistry and Imaging. Adult male Sprague–Dawley rats (250–300 g) were housed two or three per cage in environment-controlled rooms, with free access to water and food at all times. All animal handling and procedures were approved by the Salk Institute's Institutional Animal Care and Use Committee. Rats were anesthetized with chloral hydrate (350 mg/kg) administered intraperitoneally. Anesthetized rats were then perfused through the ascending aorta with saline, followed by 600–700 mL of 4% paraformaldehyde in 0.1 M borate buffer (pH 9.5). Fixative was administered for ∼20 min via a peristaltic pump. Fixed brains were then postfixed for 2 h in the same fixative used for perfusion. Brains were transferred to a 15% sucrose solution and stored overnight for cyroprotection. On the next day, the brains were frozen in dry ice and sectioned into series of 30-μm-thick coronal sections using a freezing microtome. Free-floating sections were then stored in cryoprotection buffer at −20 °C until immunohistochemical processing. Free-floating coronal sections were rinsed in KPBS and incubated for 48 h in the appropriate combination of primary antibodies diluted in KPBS supplemented with 0.3% Triton and 2% normal goat serum. Antibodies included SNX27 (1:1,000), GFAP (1:2,000; Advanced ImmunoChemical 031223), NeuN (1:5,000; Chemicon International MAB377), MAP-2 (1:200; Sigma-Aldrich M4403), PSD95 (1:2,000; Affinity BioReagents MA1-045). After primary incubation, sections were rinsed in KPBS and then incubated for 2 h using the following fluorophore-conjugated secondary antibodies (1:200, Molecular Probes): rabbit Alexa Fluor 488 (A- 21206), mouse Alexa Fluor 647 (A-21463), and guinea pig (A-21450). After secondary incubation, sections were rinsed in KPBS, mounted on gelatin-coated slides, and cover-slipped. Slides were imaged by laser confocal microscopy on a Zeiss LSM5 PASCAL laser scanning microscope under 10×, 25×, 40× (oil immersion), and 63× (oil immersion) lenses using HeNe and argon lasers. For comparison of control and antibody staining, parameters including gain, pinhole size, and percent transmission were held constant. To assess antibody specificity, SNX27 antibody was preincubated overnight at 4 °C under constant agitation with its cognate peptide. SNX27 was blocked at a concentration of 1:3,000 with peptide concentrations of 1.0 mg/mL Antibody in control sections were preincubated without peptide and stored at 4 °C under constant agitation overnight.

Molecular Biology. ***His_8 PDZ constructs.*** Constructs containing PDZ domain were cloned into the pHis8-3 vector (a derivative of pET28a vector) to contain the His_8 tag on the N terminus. The PSD95-PDZ1,2 construct encoded residues 62..249 of rat PSD95 (GenBank accession no. NP_062567). SNX27-PDZ contained residues 39..149 of rat SNX27 (GenBank accession no. NP_690060). SNX27-PDZ-ESESKV contained residues 39..133 followed by GIRK3 carboxyl terminal sequence -ESESKV (GIRK3 residues 388..393; GenBank accession no. AAB95433).

GST constructs for protein in vitro binding assay. IRK1 and GIRK3 carboxyl terminal constructs were cloned into pGEX-2T vector and contained the GST sequence followed by the cytoplasmic tail of the channel (5). The IRK1 construct contained residues 354..428 of rat IRK1 (GenBank accession no. AAB88795), and the GIRK3 construct contained residues 331..393 (GenBank accession no. AAB95433).

Full-length constructs. For electrophysiological studies, full-length channels and SNX27b were cloned into mammalian expression vector pcDNA3.1(+) (Invitrogen). PSD95 was in GWI-CMV vector (British Biotechnology), kindly provided by M. Sheng. For cell imaging clustering studies, full-length coding sequences of the GIRK3 or IRK1 were engineered to contain enhanced CFP fused to the N-terminal domain and SNX27b or PSD95 fused to enhanced YFP on the carboxyl terminal end. YFP-tagged constructs were cloned into pEYFP-N1 vector (Clontech), whereas CFP-tagged channels were cloned into pEYFP-N1 vector modified with a stop codon to inhibit expression of vector eYFP.

Site-directed mutagenesis. Point mutations were introduced using the QuikChange XL PCR-based in situ mutagenesis kit (Agilent) according to the manufacturer's instructions. The sequence of all constructs was confirmed by automated sequencing.

Cell Culture and Genetic Manipulations. ***HEK293T and COS7.*** Both HEK293T and COS7 were maintained according to a standard cell culture protocol in DMEM (Mediatec) supplemented with 10% FBS (Invitrogen) in a humidified 37 °C incubator with 5% CO_2. Cells were transiently transfected with indicated amounts of cDNA using Lipofectamine 2000 (Invitrogen) following the manufacturer's protocol. Expression was analyzed 48 h after transfection by electrophysiology or microscopy.

Rat hippocampal neurons. Primary rat hippocampal neurons were isolated from rat pups 0–2 d after birth (P0–P2) (6). Pups were anesthetized with isoflurane and killed by decapitation, after which their brains were dissected on ice. Dissected hippocampi were digested with 200 IU of papain (Worthington) for 20 min, followed by inhibition of the papain activity with trypsine inhibitor and BSA. Cells were dispersed with gentle pippetting and plated on poly-D-lysine–coated 12-mm cover glasses in plating medium (Optimem + 10 mM glucose) for 2 h. The medium was then changed to the culture medium (Neurobasal + B27 supplement + 1% penicillin/streptomycin; Invitrogen). Cultured neurons were maintained for up to 21 d in vitro; 50% of the medium volume was changed once a week. Neurons were cultured for 4–5 days in vitro (DIV) and transfected with pBOB lentivirus carrying SNX27b-YFP or GFP under control of the CamKII promoter.

Protein Expression and Purification. Recombinant protein constructs were expressed in BL21DE3 *Escherichia coli.* In brief, the bacteria were grown in 2×YT medium at 37 °C with vigorous shaking until an OD_{600nm}∼0.6 was achieved. Then the temperature was lowered to 28 °C, and protein expression was induced with 400 μM IPTG over 3 h. Bacteria cultures were spun down and kept at −80 °C until protein isolation occurred. Bacteria pellets were thawed on ice and resuspended in the lysis buffer [500 mM NaCl, 5 mM Tris (pH 8.0), 10% glycerol, and 7 mM 2-mercaptoethanol] and sonicated at low power output. Lysates were cleared from the debris by centrifugation. His_8-tagged proteins from the supernatant were immobilized on NiNTA beads (Qiagen) during a 1-h incubation at 4 °C. Beads were intensively washed with wash buffer [50 mM NaH_2PO_4, 300 mM

NaCl, 20 mM imidazole (pH 8.0)] and His_8-tagged proteins eluted from NiNTA beads using elution buffer (wash buffer with 250 mM imidazole). GST-fused channels were captured on glutathione agarose beads (Pharmacia), washed with PBS, and eluted with 10 mM reduced glutathione in 100 mM Tris (pH 7.5). The protein concentration was quantified by the Quick Start Bradford Protein Assay (BioRad) using a γ-globulin protein standard and by absorbance at 280 nm.

In Vitro Protein–Protein Binding Assay. For this assay, 2 μg of purified GST-fused channel proteins was separated by SDS/PAGE, transferred onto nitrocellulose membrane, and stained with Ponceau S to visualize proteins. Membranes were blocked with blocking buffer containing 2.5% BSA in TBST [25 mM Tris (pH 7.4), 150 mM NaCl, 2 mM KCl, 0.05% Tween-20] and incubated overnight at 4 °C, and then probed with His_8-PDZ protein (250 nM for His_8-PSD95-PDZ1,2 and 500 nM of SNX27-PDZ constructs) in blocking buffer for 1 h at room temperature. Protein–protein interaction was detected by incubation with HRP-conjugated anti-His_6 antibodies (Pierce; 1:2,500 dilution in TBST) and chemiluminescence using SuperSignal ECL reagents (Pierce). Blots were quantified by measuring the OD of anti-His_6 band and normalized by the OD of the Ponceau S band, which adjusted for differences in transfer and estimation of total protein. GST alone was used as a control for nonspecific binding.

Electrophysiology. WT and mutated channels were expressed heterologously in HEK293T cells (0.1 μg for IRK1 channels and 0.2 μg for GIRK1 and GIRK3) and together with 0.02 μg eYFP to identify positively transfected cells. Empty pcDNA3.1(+) vector was used in control transfections instead of SNX27b. For GIRK experiments, 0.4 μg of M2 muscarinic receptor was co-transfected together with channels. IRK1 currents were measured in 5K external solution containing 5 mM KCl, 155 mM NaCl, 0.5 mM $CaCl_2$, 2 mM $MgCl_2$, and 10 mM Hepes (pH 7.4). GIRK currents were measured in 20K external solution [20 mM KCl, 140 mM NaCl, 0.5 mM $CaCl_2$, 2 mM $MgCl_2$, and 10 mM Hepes (pH 7.4)]. Recording pipettes were pulled from borosilicate glass and had a resistance of 4–7 MΩ when filled with internal solution [130 mM KCl, 20 mM NaCl, 5 mM EGTA, 2.56 mM K_2ATP, 5.46 mM $MgCl_2$, 0.30 mM Li_2GTP, and 10 mM Hepes (pH 7.4)]. To record GIRK currents in neurons, the 20K solution was supplemented with 100 μM APV [(2*R*)-amino-5-phosphonopentanoate], 10 μM CNQX (6-cyano-7-nitroquinoxaline-2,3-dione) and 50 μM picrotoxin to inhibit NMDA, AMPA, and $GABA_A$ receptors, respectively. Currents were elicited with a voltage ramp protocol (200-ms duration) from −100 mV to +50 mV for GIRK currents, from −120 mV to +50 mV for IRK currents, and from +20 mV to −120 mV for neuron measurements. All protocols were delivered every 2 s. Ionic currents were measured in whole-cell configurations of the patch-clamp method. Series resistance and membrane capacitance were compensated for. Measurements were filtered at 1 kHz and sampled at 10 kHz. Data collection and analysis were done using pClamp software (Molecular Devices). All measurements were done at room temperature (22–25 °C).

Clustering Assay. COS7 cells were transfected with 0.2 μg of CFP-tagged channel and 1.0 μg of YFP-PSD95 or YFP-SNX27b. After 48 h, the cultures were washed with PBS with Mg^{2+} and Ca^{2+} and imaged by TIRF microscopy at room temperature, as described previously (7).

Crystallization and Structure Solution. Proteins for crystallization were purified by metal affinity chromatography (using NiNTA resin; Qiagen) followed by removal of His_8 tags by thrombin cleavage (Thrombin Cleavage Capture Kit; Novagen). Proteins were dialyzed overnight against a low-salt solution [30 mM NaCl, 20 mM Bis Tris (pH 6.5)]. Crystallization screening was performed using Hampton Classic Screen HR2-110 (Hampton Research) by the hanging drop diffusion method, with 1 μL of concentrated protein solution (15–25 mg/mL) mixed with 1 μL of the screening solution and incubated at 25 °C.

SNX27-PDZ-ESESKV (PDB ID code 3QE1). The diffraction-quality crystals were grown in solution containing 0.2 M $CaCl_2$*$2H_2O$, 0.1 M Hepes (pH 7.5), and 28% (vol/vol) PEG 400. The crystals were flash-frozen in liquid nitrogen directly from the drop. The data were collected at the home copper source using a Rigaku Micromax 007 diffractometer (λ = 1.54 Å) and reduced by HKL2000 (8). The structure was solved by the molecular replacement method (9) using the crystal structure of the first PDZ domain of human NHERF-2 (PDB ID code 2OCS) as the model in Phaser. The final models were built in Coot (10) and refined in RefMac (CCP4 program suite) (11).

SNX27-PDZ-GGESESKV (PDB ID code 3QDO). Crystals were grown using the hanging drop method [crystallization conditions, 0.2 M $CaCl_2$*$2H_2O$, 0.1 M Hepes (pH 7.5), 28% PEG 400]. The crystals were flash-frozen in liquid nitrogen directly from the drop. Data were collected at the Stanford Synchrotron Radiation Lightsource (beamline 9-2) and processed by HKL2000 (8). The previously determined structure of SNX27-PDZ-ESESKV was used as the model in molecular replacement. The final models were built in Coot (10) and refined in RefMac (CCP4 program suite) (11).

SNX27-PDZ complexed with free ESESKV peptide (PDB ID code 3QGL). Crystals were grown in crystallization solution containing 4.0 M sodium formate, then flash-frozen in liquid nitrogen directly from the drop. Data were collected at the Stanford Synchrotron Radiation Lightsource (beamline 9-2) and processed by HKL2000 (8). The previously determined structure of SNX27-PDZ-ESESKV was used as the initial model in molecular replacement by Molrep from the CCP4 program suite. Five monomers in an asymmetric unit cell were refined with NCS constraints and with TLS groups by Refmac (CCP4 program suite) (11).

Interestingly, the crystallographic packing was different for these three structures (Fig. S3*A* and Table S2). In both structures with a tethered ligand, the ligand sequence was bound to the neighboring SNX27-PDZ within the asymmetric unit. For SNX27-PDZ-ESESKV, the PDZ domain ligand forms an infinite linear polymer, whereas for SNX27-PDZ-GG-ESESKV it forms dimers.

Molecular Graphics. Images of PDZ structures and their ligands, as well as maps of electrostatic potentials on their molecular surfaces, were produced using PyMol (DeLano Scientific), APBS plug-in (12), Molscript (13), and MolMol (14).

Structure Alignments. Alignment of PDZ domains for rat PSD95 (UniProt P31016) and SNX27 (UniProt Q8K4V4) were done using the ClustalV algorithm (15).

Statistical Analysis. Data are presented as mean ± SEM. Statistical significance was assessed using an unpaired Student *t* test for two groups and one-way ANOVA followed by the Dunnett post hoc test for three or more groups using GraphPad Prism 5.0 (GraphPad Software). A P value <0.05 was considered statistically significant.

1. Joubert L, et al. (2004) New sorting nexin (SNX27) and NHERF specifically interact with the 5-HT4a receptor splice variant: Roles in receptor targeting. *J Cell Sci* 117: 5367–5379.
2. Rincón E, et al. (2007) Proteomics identification of sorting nexin 27 as a diacylglycerol kinase zeta-associated protein: New diacylglycerol kinase roles in endocytic recycling. *Mol Cell Proteomics* 6:1073–1087.
3. MacNeil AJ, Mansour M, Pohajdak B (2007) Sorting nexin 27 interacts with the Cytohesin-associated scaffolding protein (CASP) in lymphocytes. *Biochem Biophys Res Commun* 359:848–853.
4. Lauffer BE, et al. (2010) SNX27 mediates PDZ-directed sorting from endosomes to the plasma membrane. *J Cell Biol* 190:565–574.
5. Lunn ML, et al. (2007) A unique sorting nexin regulates trafficking of potassium channels via a PDZ domain interaction. *Nat Neurosci* 10:1249–1259.
6. Nassirpour R, et al. (2010) Morphine- and CaMKII-dependent enhancement of GIRK channel signaling in hippocampal neurons. *J Neurosci* 30:13419–13430.
7. Fowler CE, Aryal P, Suen KF, Slesinger PA (2007) Evidence for association of GABA(B) receptors with Kir3 channels and regulators of G protein signalling (RGS4) proteins. *J Physiol* 580:51–65.
8. Otwinowski Z, Minor W (1997) Processing of X-ray diffraction data collected in oscillation mode. *Methods in Enzymology*, eds Carter CW, Sweet RM (Academic Press, San Diego, CA) vol 276, pp 307–326.
9. Rossmann MG (1990) The molecular replacement method. *Acta Crystallogr A* 46: 73–82.
10. Emsley P, Cowtan K (2004) Coot: Model-building tools for molecular graphics. *Acta Crystallogr D Biol Crystallogr* 60:2126–2132.
11. Collaborative Computational Project, Number 4 (1994) The CCP4 suite: Programs for protein crystallography. *Acta Crystallogr* 50:760–763.
12. Baker NA, Sept D, Joseph S, Holst MJ, McCammon JA (2001) Electrostatics of nanosystems: Application to microtubules and the ribosome. *Proc Natl Acad Sci USA* 98:10037–10041.
13. Kraulis P (1991) MOLSCRIPT: A program to produce both detailed and schematic plots of protein structures. *J Appl Cryst* 24:946–950.
14. Koradi R, Billeter M, Wuthrich K (1996) MOLMOL: A program for display and analysis of macromolecular structures. *J Mol Graphics*, 14:51–55.
15. Higgins DG (1994) CLUSTAL V: Multiple alignment of DNA and protein sequences. *Methods Mol Biol* 25:307–318.

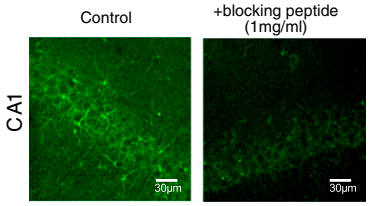

Fig. S1. Specificity of the pan anti-SNX27 antibody for immunofluorescence staining. The CA1 region of rat hippocampus section stained with rabbit pan anti-SNX27 (SNX27a/b) antibody alone (*Left*) or pan anti-SNX27 antibody preincubated with 1 mg/mL of blocking peptide (M1-G18 amino acids of rat SNX27, used previously as epitope for antibody production). The addition of blocking peptide reduces staining to background levels, confirming specificity of binding.

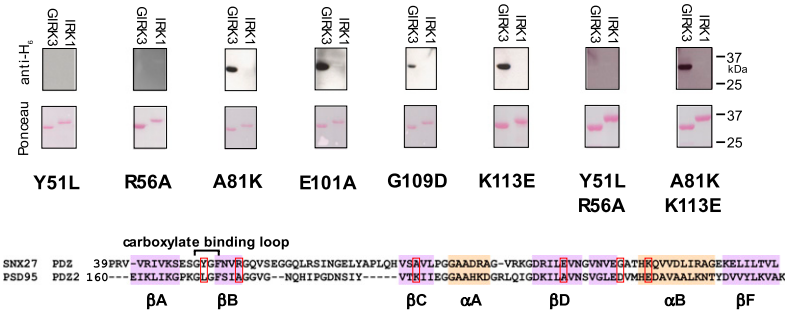

Fig. S2. Point mutations in SNX27-PDZ that disrupt binding to GIRK3. Protein overlay blots show the results of testing the binding of the SNX27-PDZ point mutants to GIRK3 and IRK1. Notably, Y51L and R56A mutations in the PDZ domain disrupted the binding to the both GIRK3 and IRK1. Other mutants displayed interaction with GIRK3 tail, and no mutants showed any detectable binding to IRK1.

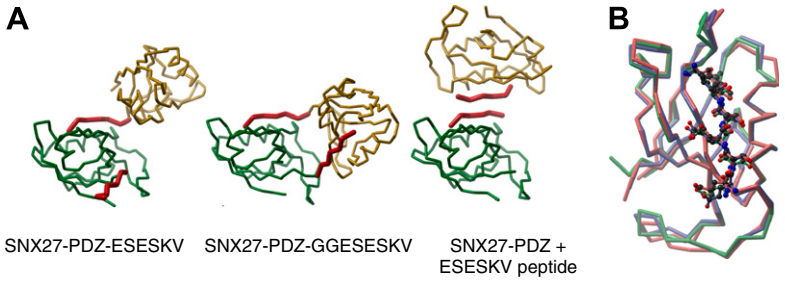

Fig. S3. Comparison of different crystal structures of SNX27-PDZ bound to GIRK3 carboxyl terminal ligand. (*A*) Structural determination of three SNX27-PDZ variants (SNX27-PDZ-ESESKV, SNX27-PDZ-GGESESKV, and SNX27-PDZ with free *N*-acetyl-ESESKV-COOH peptide; *Results* and *Materials and Methods*). Note the protein structures are in different crystallographic spaces, but have similar backbone structures (Table S2). Dark-red color indicates ESESKV peptide, and SNX27-PDZ structures are shown in green and gold. (*B*) Alignment of the backbone structures for SNX27-PDZ-ESESKV (green) SNX27-PDZ-GGESESKV (red), and SNX27-PDZ plus free ESESKV peptide (blue) reveals very similar structures, including the βB–βC loop conformation and position of the peptide ligand. Atom positions of main and side chains of the bound ligand for all three structures are shown as well.

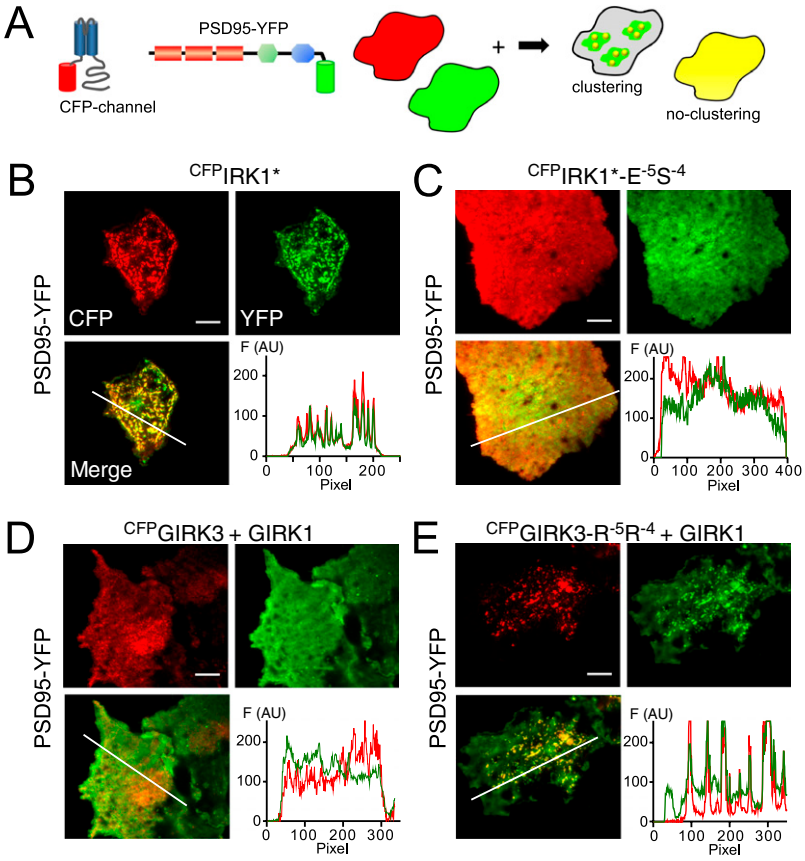

Fig. S4. Mutation of −5 and −4 positions reverses association and functional regulation of IRK1 and GIRK1/3 channels by PSD95. (*A*) Cartoon illustrating the design of the clustering assay with PSD95. Proteins expressed alone exhibit a diffuse pattern of localization on the cell surface but form clusters when the channel is coexpressed with PSD95. CFP is pseudo-colored red and YFP is green. (*B–D*) Fluorescent images show coclustering of ion channels and PDZ proteins expressed in COS7 cells. Images were collected using TIRF microscopy. N-terminal–tagged IRK1* (^{CFP}IRK1* and ^{CFP}IRK1*-E^{-5}S^{-4}) was coexpressed with PSD95-YFP. ^{CFP}IRK1* (*B*), but not ^{CFP}IRK1*-E^{-5}S^{-4} (*C*), forms large clusters with PSD95-YFP. Plots on right show fluorescence intensity of CFP and YFP measured at the white line in the merged image. (*D* and *E*) N-terminal–tagged GIRK3 (^{CFP}GIRK3 and ^{CFP}GIRK3-R^{-5}R^{-4}) was coexpressed with GIRK1 and PSD95-YFP. ^{CFP}GIRK3-R^{-5}R^{-4} (*E*), but not ^{CFP}GIRK3 (*D*), forms numerous clusters with PSD95-YFP. (Scale bar: 10 μm.)

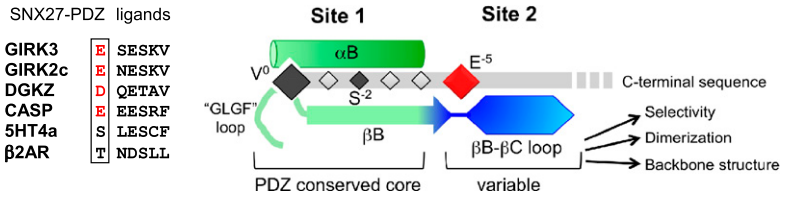

Fig. S5. Model for SNX27-PDZ binding selectivity. Alignment of SNX27-associating ligands, which contain a negatively charged Glu or polar Ser or Thr at the −5 position and Val, Leu, or Phe at the 0 position: 5HT4a serotonin receptor class 4a (1), diacylglycerol kinase zeta (DGKZ) (2), cytohesin-associated scaffolding protein (CASP) (3), and β2 adrenergic receptors (β2AR) (4). (*Right*) A two-site model for PDZ selectivity. One site involves the canonical PDZ binding motif for SNX27 Val (or Phe, Leu) in position 0, necessary for binding to SNX27-PDZ. The second site is formed by the βB–βC loop and associates electrostatically with a negative charge (or neutral) on the −5 residue but repels a positive charge of IRK1. The second site might have evolved to fine-tune PDZ selectivity or perform other functions for the PDZ-containing protein.

Table S1. Effects of SNX27b expression on potassium currents in neurons and HEK293T cells

	Control		+SNX27b	
Neurons				
Baclofen-induced current	−24.98 ± 4.70	(n = 10)	−9.68 ± 2.20**	(n = 12)
Ba^{2+}-sensitive basal current	−18.22 ± 2.98	(n = 10)	−7.82 ± 1.35**	(n = 12)
HEK293T				
Ba^{2+}-sensitive basal current				
IRK1*	−189 ± 19	(n = 12)	−285 ± 39*	(n = 11)
IRK1*-$E^{-5}S^{-4}$	−461 ± 76	(n = 12)	−268 ± 40*	(n = 15)
Carbachol-induced current				
GIRK3/GIRK1	−48.5 ± 7.5	(n = 13)	−20.7 ± 3.7*	(n = 14)
GIRK3-$R^{-5}R^{-4}$ /GIRK1	−23.8 ± 7.2	(n = 8)	−35.2 ± 7.7	(n = 10)

For neuronal recordings, baclofen current is defined as the difference between the current recorded in 20 mM K^+ + 100 μM baclofen and the current in 20 mM K^+ external solution. Ba^{2+}-sensitive basal current is defined as difference between the current in 20 mM K^+ solution and the current in 20 mM K^+ with 1 mM Ba^{2+}. Controls are neurons infected with GFP-expressing virus. For HEK293T cells, IRK1* mutant currents are Ba^{2+}-sensitive basal current, defined as the difference between current in 5 mM K^+ solution and the current in 5 mM K^+ with 1 mM Ba^{2+}. GIRK currents are carbachol-induced currents, defined as the difference between the current in 20 mM K^+ + 100 μM baclofen and the current in 20 mM K^+ external solution alone. Controls are HEK293T cells transfected with empty pcDNA3.1 vector. Values are mean ± SEM. Statistical significance vs. control, $^{**}P < 0.01$; $^{*}P < 0.05$.

Table S2. Crystallographic data and refinement statistics of SNX27 PDZ crystal structures

	SNX27-PDZ-ESESKV (PDB ID code 3QE1)	SNX27-PDZ-GG-ESESKV (PDB ID code 3QDO)	SNX27-PDZ + free ESESKV peptide (PDB ID code 3QGL)
Data collection			
Space group	H3	I41	P21
Cell dimensions			
a, *b*, and *c*, Å	75.789, 75.789, 40.939	59.795, 59.795, 53.606	45.571, 81.567, 90.678
α, β, and γ, degrees	90.00, 90.00, 120.00	90.00, 90.00, 90.00	90.00, 102.11, 90.00
Resolution, Å	50.00–1.68 (1.68–1.71)*	50.00–1.88 (1.88–1.93)*	50.00–3.30 (3.30–3.36)*
R_{sym}	0.039 (0.174)*	0.045 (0.106)*	0.093 (0.208)*
$I/\sigma I$	39.53 (6.68)*	37.30 (19.40)*	14.72 (6.08)*
Completeness, %	89.1 (45.2)*	99.8 (100)*	99.8 (98.3)*
Redundancy	4.8 (3.3)*	7.2 (7.2)*	3.8 (3.5)*
Refinement			
Resolution, Å	37.90–1.68	42.28–1.88	38.95–3.31
Number of reflections	8503	7380	9329
R_{work}/R_{free}	0.158/0.223	0.144/0.203	0.225/0.254
Nonhydrogen atoms, n			
Protein	762	798	3815
Ligand/ion	—	—	—
Water	120	108	5
B factors			
Protein	19.983	18.388	47.026
Ligand/ion	—	—	—
Water	30.537	24.149	24.533
RMSD			
Bond lengths, Å	±0.024	±0.023	±0.010
Bond angles, degrees	±1.976	±2.020	±1.207

*The highest-resolution shell is given in parentheses.